frontiers | Frontiers in Earth Science

TYPE Original Research
PUBLISHED 16 January 2023
DOI 10.3389/feart.2022.1048042

OPEN ACCESS

EDITED BY
Zhenzhi Wang,
Henan Polytechnic University, China

REVIEWED BY
Chong Xu,
Guizhou Education University, China
Bing Jia,
Henan University of Urban Construction, China
Yanjun Meng,
Taiyuan University of Technology, China

*CORRESPONDENCE
Zhigang Du,
gangduzhi@163.com

†These authors have contributed equally to this work and share first authorship

SPECIALTY SECTION
This article was submitted to Economic Geology, a section of the journal Frontiers in Earth Science

RECEIVED 19 September 2022
ACCEPTED 20 October 2022
PUBLISHED 16 January 2023

CITATION
Huang Q, Du Z, Liu H, Niu Q, Fang H, Yang J and Lou M (2023), Investigation of cleat and micro-fracture and its aperture distribution in the coals of different ranks in North China: Relative to reservoir permeability.
Front. Earth Sci. 10:1048042.
doi: 10.3389/feart.2022.1048042

Investigation of cleat and micro-fracture and its aperture distribution in the coals of different ranks in North China: Relative to reservoir permeability

Qiang Huang[1†], Zhigang Du[1,2*†], Hewu Liu[3], Qinghe Niu[4], Huihuang Fang[3], Jinyang Yang[1] and Minghang Lou[1]

[1]School of Civil Engineering, Luoyang Institute of Science and Technology, Luoyang, China, [2]Yima Coal Corporation, Henan Energy Group Corporation, Sanmenxia, China, [3]School of Earth and Environment, Anhui University of Science and Technology, Huainan, China, [4]State Key Laboratory of Mechanical Behavior and System Safety of Traffic Engineering Structures, Shijiazhuang Tiedao University, Shijiazhuang, China

The apertures of cleats and micro-fractures in coal play an important role in the permeability of the coal bed. In this study, optical microscopy and scanning electron microscopy were used to investigate the morphology of cleats and micro-fractures and their apertures, distribution of minerals, and matrix/fracture interactions. The neighboring mineralized and unmineralized cleats suggest the possibility of multi-stage evolutionary processes of cleat formation during the coalification process. The micro-fracture distribution of coals is closely related to their components, including organic macerals and inorganic minerals. Micro-fractures are prone to developing at the junction surface of organic macerals or the surface of organic and inorganic minerals. A mineral-genetic micro-fracture can be classified as an intra-crystal micro-fracture, an extra-crystal micro-scale fracture, or a grain-edge micro-scale fracture. Compared with the low- and middle-ranking coals, cleat and micro-scale fractures in high-ranking coal are usually filled with carbonate minerals and clay minerals. Statistical analysis reveals that the aperture distribution of cleat and micro-fracture in coal shows a log-normal distribution. The aperture of cleat and micro-fracture shows a decreasing trend with increase in coal rank. For low-ranking coal, cleats contribute more to the permeability than micro-fractures. However, for the middle- and high-ranking coals, the contribution of cleats and micro-fractures to the coal reservoir permeability will be close. As the rank of coal increases, the degree of cleat contribution to reservoir permeability decreases, while the degree of micro-fracture contributing to the reservoir permeability increases. Possible reasons for the extremely low reservoir permeability in China may be the following: 1) subsurface cleats and micro-fractures close their apertures significantly due to the *in situ* geo-stress or 2) cleats and micro-fractures have better permeability in the geological history, which makes the precipitation of minerals decrease the coal reservoir permeability. Therefore, the acid solvent (e.g., HAc, HCl, and HF) added to the drilling or hydraulic fracturing fluid or the geo-stress relief technologies may be an effective way of enlarging the cleat or micro-fracture aperture and enhance the reservoir permeability for coalbed methane production.

KEYWORDS
coal, cleat, micro-fracture, permeability, statistical analysis

Introduction

In coal, fractures form the primary seepage passage for coalbed methane (CBM) migration out of the coalbed, which plays an essential role in the successful production of CBM (Heriawan and Koike, 2015; Weniger et al., 2016; Zhang et al., 2016; Shi et al., 2018; Wang et al., 2018; Wang et al., 2021; Du et al., 2022). At present, enhanced measures commonly used in the development of CBM production, including the technology of hydraulic fracturing or foam fracturing, are primarily intended to create fracture channels or fracture networks in the coalbed.

Due to the importance of fractures in coal, scholars have performed extensive investigations into the fracture attributes, including the aperture, appearance, extension, and distribution characteristics. Usually, cleats refer to systematic fractures in coal beds since miners adopted the term in the early 19th century (Kendall and Briggs, 1933). In all the factors that can affect the gas transport of CBM production, the permeability of cleat systems has the most influence (Niu et al., 2021; Du et al., 2022). Pan et al. (2014) noted that cleats are usually restricted to a single lithotype, while fractures can cross different lithotypes. Cleat apertures between 4 μm and 50 μm may be optimal for CBM production, based on the San Juan Basin coals. Larger apertures may lead to high permeability as well as high water production, which is detrimental to economic production (Scott, 2002). Sapiie et al. (2014) applied 2D and 1D methods to determine the distributions of cleat spacing and found a power-law relationship in Indonesian coal cleats. Cleat apertures in the subsurface are smaller than in unstressed surface samples, but core samples at the surface approximate the aperture.

With the development of advanced testing technology, the contribution of micro-fracture to the permeability of coalbed has attracted the attention of many scholars. Gamson et al. (1993) studied the low- and middle-ranking coals in the Bowen Basin, Australia. They defined micro-fractures in the coal as those that are invisible to the naked eye and that have an aperture of 0.05–20 μm and micro-permeability. Karacan and Okandan (2000) studied middle-ranking coal in the Zonguldak Basin of Turkey and found that the micro-fractures often communicate with the cleats in the coal. Yao et al. (2010) studied mass samples (including low-, middle-, and high-ranking coals) in North China and found that the micro-fracture density in the coal is closely related to the rank of the coal. Gong et al. (2010) used CT image analysis technology and found that the micro-fracture aperture in the coal can reach 182.62 μm. Kumar et al. (2011) proposed using microwave energy to induce fractures and increase cleat apertures in coal. Mohamad and Katsuaki (2015)studied low-ranking coal in Indonesia and concluded that the micro-fracture development in coal is closely related to the mineral components. Taking coals suffering from different degrees of geological deformation, Du et al. (2019) examined the permeability of cleats and micro-fractures in the coal using statistical methods and found that the permeability of the cleat (about 1–100 mD) was much larger than that of the micro-fracture (about 0.01–1 mD).

On the whole, earlier works have conducted a wide range of research studies on fractures in coal. In addition to the study of cleats, research on micro-fractures is increasingly active in recent years. Quantitative approaches have been used to express the relationship between coal fractures and permeability. In the classical permeability parallel-plate fracture model, the permeability of the coal can be written as follows:

$$k = \frac{(84.4 \times 10^5)x^3}{s}, \quad (1)$$

where k is fracture permeability (D), x is the aperture of the fracture between two fracture surfaces (cm), and s is the fracture space. This relationship indicates that the fracture aperture, x, has a significant influence on permeability, as it is raised to the third power of the permeability.

A better understanding of the cleat and the micro-fracture structure, especially the aperture, is essential for evaluating the permeability of the coal reservoir and the economic aspects of CBM exploration and exploitation (Nalendra et al., 2020). At present, the distribution of fracture apertures and their effects on fluid flow in the rock are attracting more attention, but little work has focused on this issue in coal (Yang et al., 2012; Rutqvist et al., 2018; Brixel, 2020). This study seeks to provide a further understanding of the fracture attribute of coal and its permeability. The experiment samples were prepared in the way described by Du et al. (2019). The cleat and micro-fracture characteristics and their aperture distribution to the coal reservoir permeability are investigated for coals of different ranks in North China. The implications of this for the CBM exploration and exploitation are also discussed.

Materials and methods

Sample collection

In this study, 50 coal samples were collected. The locations of the samples are shown in Figure 1. These include low-ranking coal from the Shendong mining area of Shaanxi Province, middle-ranking coal from the Pingdingshan mining area of Henan Province and high-ranking coal from the Qinshui Basin of Shanxi Province.

Basic coal analyses, including vitrinite reflectance measurements, petrographic composition analysis, mineral

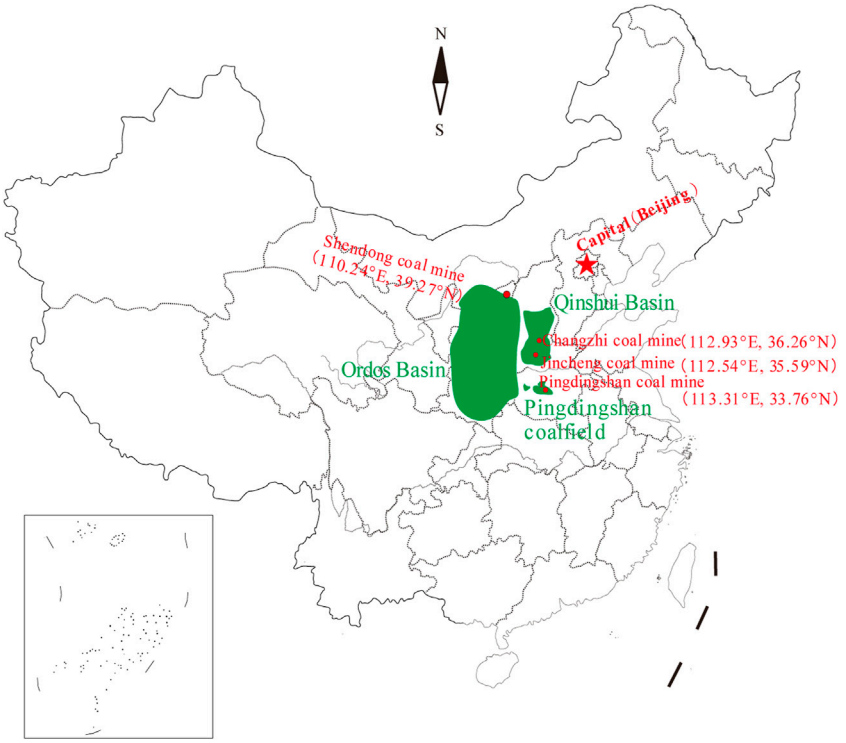

FIGURE 1
Location of sampled coals.

matter, micro-fracture frequency, and orientation determination, were performed for all these samples by using the standard methods described in the previous research (Li et al., 2015; Du et al., 2019). These methods are here briefly described. The coal blocks were crushed, and polished sections were prepared for vitrinite reflectance determination (with 500 points) and petrographic composition analysis. Chemical compositions of mineral matter were determined using SEM-EDS on naturally broken surfaces. The original micro-fracture frequency was investigated using optical microscopy.

The collected coal samples were assigned designations, as follows: Shendong sample (SD), Pingdingshan sample (PDS), and Qinshui sample (QS). In terms of coal quality (Table 1), the sulfur content in the SD and PDS samples was higher than in the QS sample. In the petrographic composition (Table 2), all of the coals mainly consisted of vitrinite maceral. A comparison shows that there was more inertinite maceral in the PDS sample. The coals were typically richer in vitrinite than inertinite macerals, with more than 80% vitrinite and 10–20% inertinite in most of the samples studied. Liptinite was usually present as only a small fraction (0–3.4%) of the macerals in three of the coals (samples B1, B3, and B4), while the others had no liptinite. The ash yield of the coals varied from 4.34% to 17.44%, and fixed carbon varied from 75.06 to 85.94%.

Sample preparation

Studies of fractures in coal have been performed with sample preparation randomly or arbitrarily by small particle samples. Due to the arbitrariness of the sample preparation, there are no reference standards to systematically classify micro-scale fractures in the coal. Cleat as endogenous fractures, formed during the process of coalification, has good continuity, and face cleat (long fracture) and butt cleat (short fracture) can be clearly distinguished in a hand specimen (Figure 2). Therefore, taking the direction of the cleat in the coal as a positioning standard, an oriented sample was prepared.

Fractures at the edge of the sample are considered damage-induced and were not used in the analysis. To minimize these fractures, the non-destructive method of a diamond wire cutting machine was used. The collected coal samples were prepared as follows: first, the oriented block samples (width 50 mm × length 80 mm × thickness 10–15 mm) were cut from the collected samples with the diamond wire cutting machine along the direction of the face cleat and butt cleat (Figure 3). The cutting speed of the diamond wire cutting machine was 0.02 m/s. The oriented samples (width 1 × length 1 × thickness 0.5 cm) were also

TABLE 1 Coal quality data of the sampled coals.

Sample	Proximate analysis (wt%, adb)				Element analysis (%)					Density 10^3 kg/m^3
	M_{ad}	A_d	V_{daf}	FC_{ad}	$S_{t.d}$	O_{daf}	C_{daf}	H_{daf}	N_{daf}	
SD	13.90	7.69	39.64	47.94	0.79	20.30	73.18	4.48	1.18	1.52
PDS	1.01	6.10	16.63	77.49	0.40	3.40	90.51	4.39	1.27	1.31
QS	1.47	8.51	5.93	84.09	0.39	4.42	90.77	3.74	0.64	1.44

TABLE 2 Petrographic composition data of the sampled coals.

Sample	Formation	$R_{o,max}$ %	Petrographic analysis (vol.%, mmf)			
			Vitrinite vol.%	Liptinite vol.%	Inertinite vol.%	Mineral vol.%
SD	Middle-lower Jurassic (J_2y)	0.56	80	1	7	12
PDS	Lower Permian (P_1sh)	1.32	74	0	19	7
QS	Lower Permian (P_1sh)	2.75	93	0	2.0	5

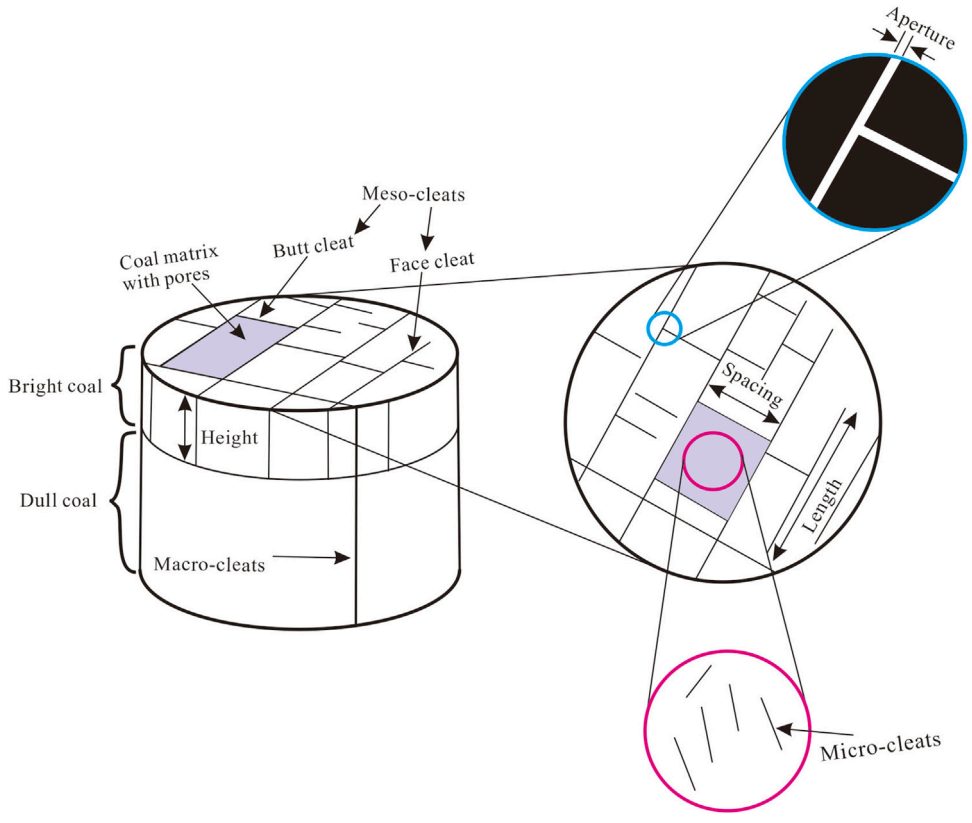

FIGURE 2
Fracture patterns in the coal (revised from Laubach et al., 1998).

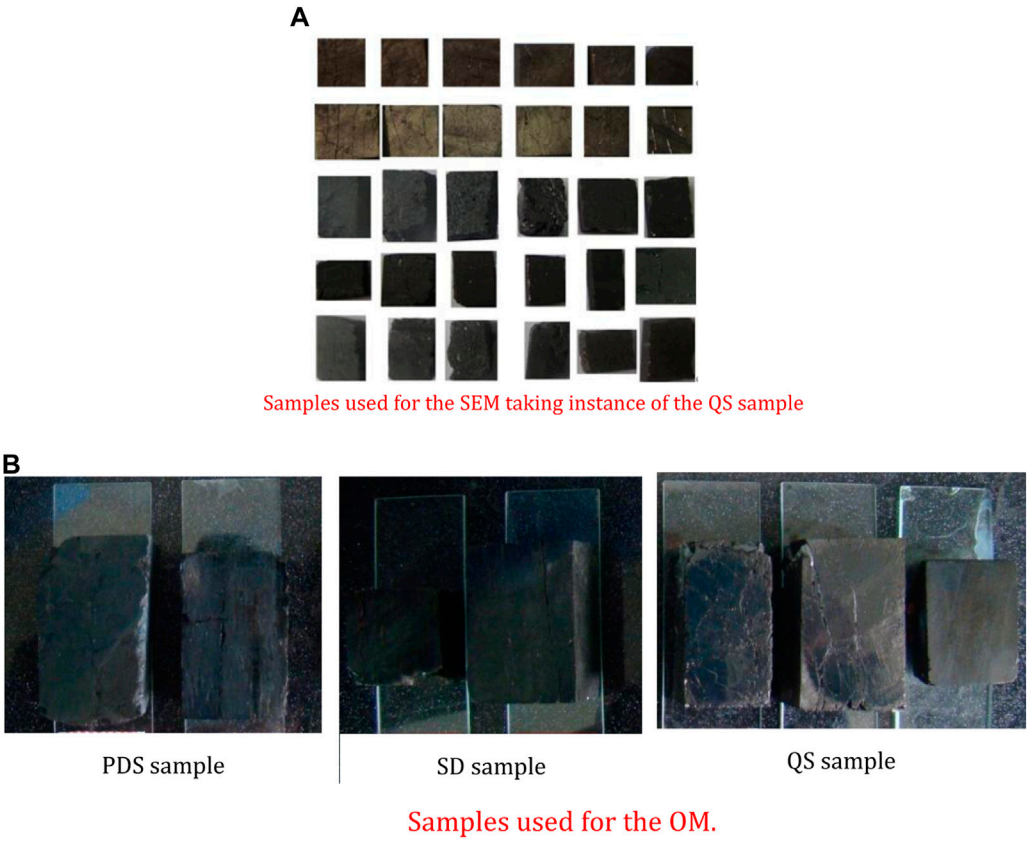

FIGURE 3
Prepared oriented coal samples.

prepared. Then, these samples were gold coated (Figure 3A) and polished (Figure 3B) for study by scanning electron microscopy (SEM) and optical microscopy (OM).

To interpret the coal micro-structure, oriented block samples are the best method of examining a small, specific part of a given sample in three dimensions: 1) the face cleat, 2) the butt cleat, and 3) the bedding. The major advantages of using this technique are that it allows observation of 1) coal micro-structure in three dimensions and therefore provides information on the shape, size, and cross-sectional area of the micro-structures and their bearings to the face and butt cleat and bedding; 2) fracture aperture, orientation, and continuity; and 3) the distribution of the micro-fracture and its relationship to the pore or cleat.

Apparatus and methods

In this study, the combined methods of OM and SEM were adopted. The OM method can be used to observe the micro-fractures in the coal. Its model is Leica DM4 P with a magnification of eyepiece 10× and a magnification of objective lens of 5×, 10×, 20×, 50×, and 100×. Then, with the eyepiece and the objective lens, a maximum magnification of 1000× imaging can be achieved. In addition, the SEM method was also adopted to study the fractures in coal. Its model is Quanta 250 with a function of magnification imaging of 1 million times. This can be taken to observe the nano-fracture in coal. An X-ray energy spectrometer is attached to this instrument, which helps recognize the minerals.

In the results section of this study, frequency diagrams of the cleat and micro-fracture aperture are compared between coals of different ranks. The fracture aperture, which contributes to the permeability of the coal reservoir, can be fitted to an appropriate probability distribution. In the case of a coal fracture aperture, several probability distributions are available to describe such data; they vary significantly in mathematical complexity and the number of parameters that require fitting. Minitab® 17, for instance, has over 20 distributions that can be readily tested. The log-normal distribution of fracture aperture of rock was previously reported by Snow (1968). According to the results

10.3389/feart.2022.1048042

TABLE 3 Probability distributions analyzed in the present work.

Distribution	Probability distribution function	Cumulative distribution function	Skewness	Kurtosis
Normal $x \sim N(\mu, \sigma^2)$	$P(x) = \frac{1}{\sqrt{2\pi}\sigma} exp\left[-\frac{(x-\mu)^2}{2\sigma^2}\right]$	$t = x^{\lambda} \text{for} \lambda \neq 0$ $C(x) = \int_0^x \frac{1}{\sqrt{2\pi}\sigma} exp\left[-\frac{(t-\mu)^2}{2\sigma^2}\right]dt$	$\nu_{1-N} = E[(x - E(x))^3]/(D(x))^{3/2}$	$\nu_{2-N} = E[(x - E(x))^4]/(\sigma(x))^{3/2}t$
Log-normal $Ln(x) \sim N(\mu, \sigma^2)$	$P(x) = \frac{1}{\sqrt{2\pi}\sigma} exp\left[-\frac{(\ln x-\mu)^2}{2\sigma^2}\right]$	$C(x) = \int_0^{\ln x} \frac{1}{\sqrt{2\pi}\sigma} exp\left[-\frac{(t-\mu)^2}{2\sigma^2}\right]dt$	$\nu_{1-L} = E[(Ln(x) - E(Ln(x)))^3]/(D(Ln(x)))^{3/2}$	$\nu_{2-L} = E[(Ln(x) - E(Ln(x)))^4]/(\sigma(Ln(x)))^{3/2}$
Square root $\sqrt{x} \sim N(\mu, \sigma^2)$	$P(x) = \frac{1}{\sqrt{2\pi}\sigma} exp\left[-\frac{(\sqrt{x}-\mu)^2}{2\sigma^2}\right]$	$C(x) = \int_0^{\sqrt{x}} \frac{1}{\sqrt{2\pi}\sigma} exp\left[-\frac{(t-\mu)^2}{2\sigma^2}\right]dt$	$\nu_{1-S} = E[(\sqrt{x} - E(\sqrt{x}))^3]/(D(\sqrt{x}))^{3/2}$	$\nu_{2-S} = E[(\sqrt{x} - E(\sqrt{x}))^4]/(\sigma(\sqrt{x}))^{3/2}t$

from the rock, the normal, logarithmic normal, and square root distributions were selected. The distributions and their transformations are listed in Table 3. All of these are two-parameter distributions, although some have three-parameter versions as well. The maximum likelihood method was used to estimate these parameters.

Results and discussion

Cleats and micro-structures in coals

Cleats commonly show little shear offset and are, therefore, opening-mode fractures (Solano et al., 2007; Sapiie et al., 2014). Previous studies of coals using scanning electron microscopy (SEM) show a range of micro-structures between the micro-pores and the cleat system. To characterize cleats and micro-structures in coals (Figure 4), a line is placed perpendicular to the cleat or micro-fracture direction. Fracture aperture is determined from the opposite fracture plane in this way.

The occurrence of nanometer-sized pores or cavities (209.2 to 456.8 nm) on the cleat suggests that it is a gas drainage passage in the transmissibility of methane from the coal matrix to the cleat. Among cleats in coal, the face cleat is the most conspicuous fracture seen in the hand specimen and penetrates the coal at right angles to the bedding. The butt cleat, in comparison, is less pervasive and is confined to areas between the face cleats and typically penetrates the coal at right angles to the face cleat and bedding. Both the face and butt cleats commonly occur as orthogonal sets, oriented perpendicular to the bedding. Characteristically, face and butt cleats are of a planar shape, varying in vertical extent or height (L-5 mm) and width (0.1–2 mm), and are usually spaced 0.3–2 mm apart. In all of the coals examined, cleats are infilled with clays, quartz, or calcite, offering little porosity and permeability, which will be discussed in detail as follows.

A cleat network can be simply classified into two orthogonal fractures (face and butt cleats). Both face and butt cleats are oriented perpendicular to bedding, but butt cleats usually abut against face cleats. Thus, face cleats are through-going, while butt cleats end at intersections with face cleats. Cleats form in response to the physical and chemical processes during coalification. Fracture growth modeling shows that this orthogonal relationship can arise under biaxial extension (Olson et al., 2009), a circumstance that can accompany the conditions under which cleats form. Laubach et al. (1998) gave a thorough review of the origins of cleats as well as a discussion of cleat-forming mechanisms. The coupling action of the fluid pressure and *in situ* stress determines the development of cleats and micro-fractures in the coal, which is also related to the coal types, rank, maceral, and coal thickness.

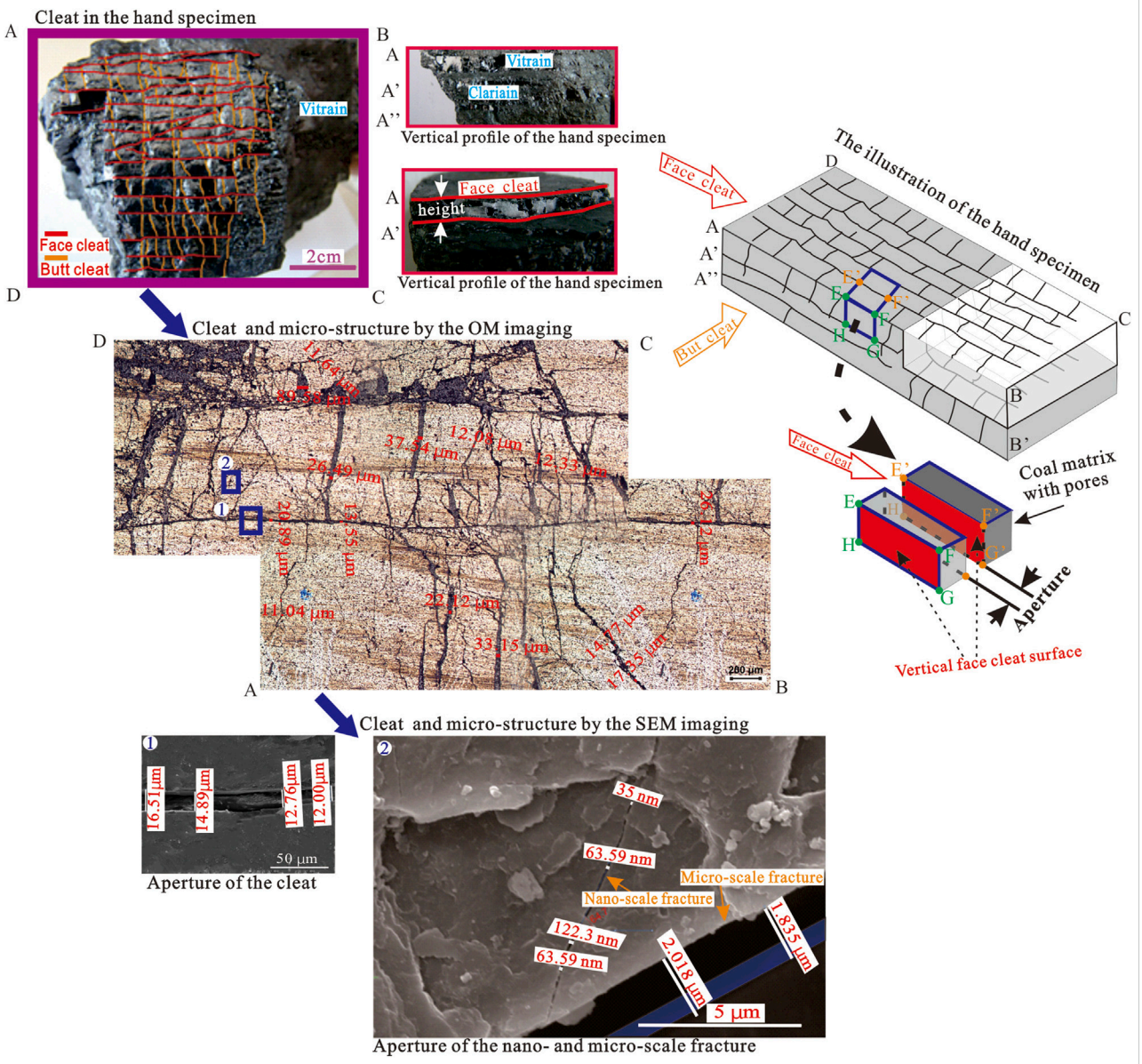

FIGURE 4
Cleats and micro-structures in coal.

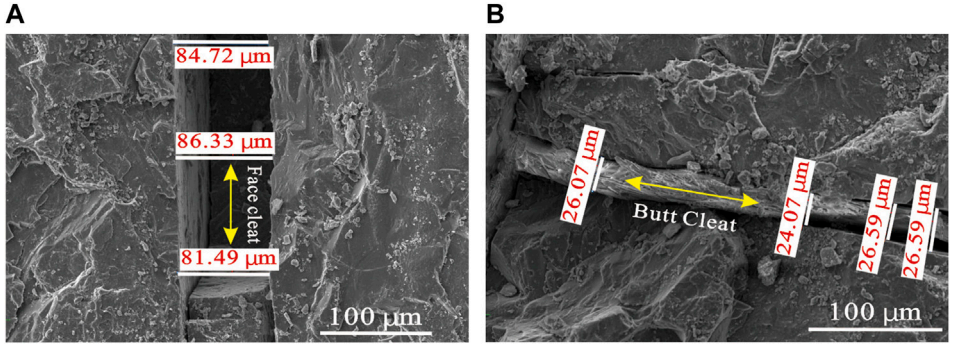

FIGURE 5
Mineralized face cleat and butt cleat: **(A)**, face cleat; **(B)** butt cleat.

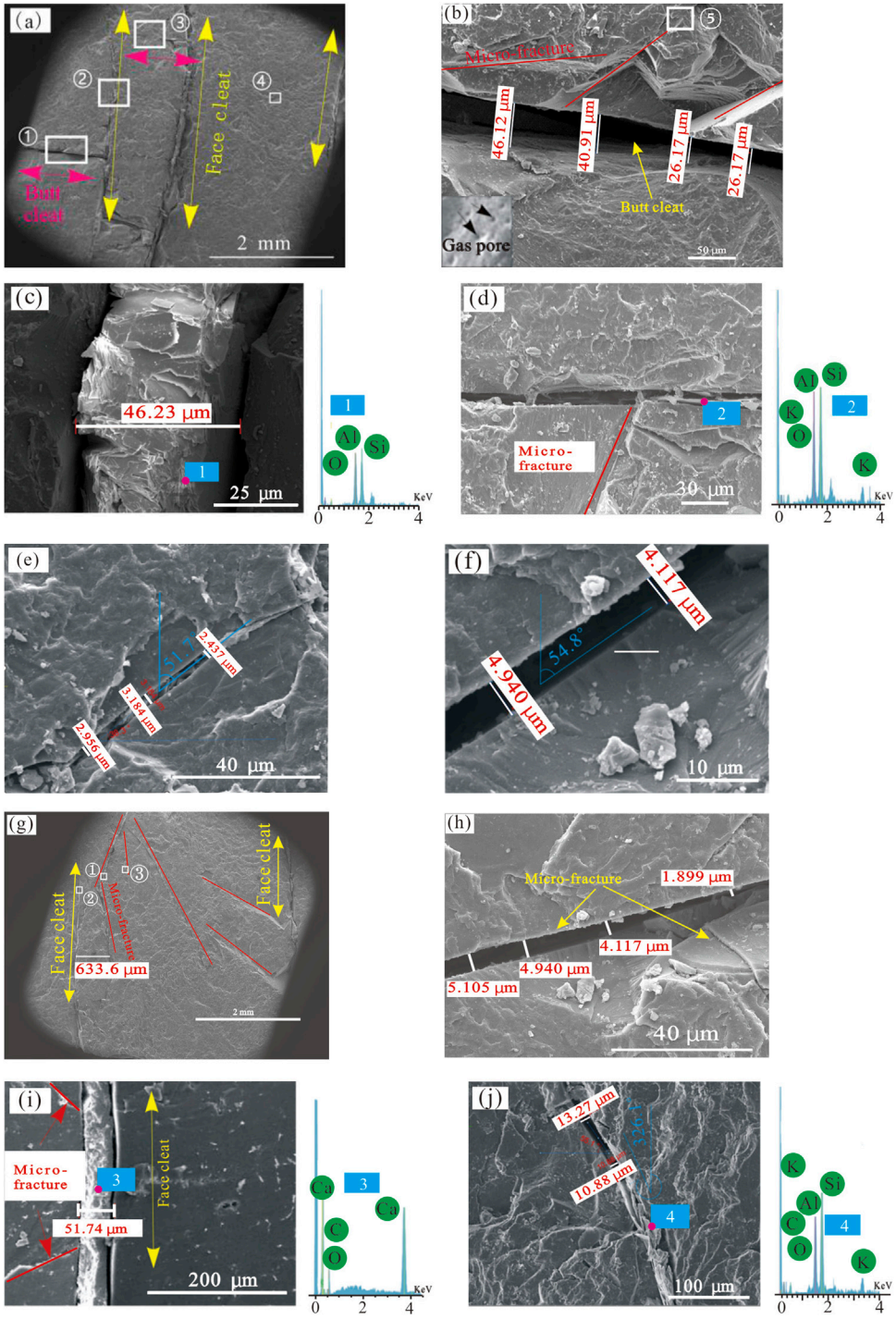

FIGURE 6
Cleat and micro-fractures in the coal: **(a)**, face cleat and butt cleat; **(b)**, enlarged view of point 1 in Figure 6(a); **(c)**, enlarged view of point 2 in Figure 6(a); **(d)**, enlarged view of point 3 in Figure 6(a); **(e)**, enlarged view of point 4 in Figure 6(a); **(f)**, enlarged view of point 5 in Figure 6(b); **(g)**, face cleat and micro-fracture; **(h)**, enlarged view of point 1 in Figure 6(g); **(i)**, enlarged view of point 2 in Figure 6(g); **(j)** enlarged view of point 3 in Figure 6(g).

Cleat and micro-fractures related to the inorganic non-metallic mineral

Figures 5A,B show the mineralized face cleat and butt cleat in the QS sample, respectively. From a genetic perspective, the mineral matter in coal, similar to the organic matter, is a product of the processes associated with coal formation, as well as changes in subsurface fluids and other aspects of sediment diagenesis (Golab et al., 2013). Cleat minerals are not intimately associated with coal, unlike detrital and early diagenetic (syngenetic) minerals. The occurrence of cleat minerals is of great importance for determining the evolution of the pore fluids and the age of the cleat itself. Cleat minerals may form due to several different processes, and the formation and migration of CBM and other hydrocarbons generated during or after coalification may also be related to mineralization (Ward, 2002, 2016). Tectonism and geothermal activity can produce hydrothermal fluids, which can result in epigenetic mineralization and alteration of diagenetic minerals within coals (Saxby, 2000; Dai et al., 2014). At least, the mineralized cleats imply that cleats had better fluid conductivity during geological history, which is beneficial for the infiltration and migration of mineralized fluids and the precipitation of minerals in the stressed cleats. This further indicates that although cleat apertures in the subsurface are smaller than in unstressed surface samples, core samples at the surface approximate the apertures (Weniger et al., 2016).

Figure 6 shows the cleat and micro-fractures related to the inorganic non-metalic mineral. The minerals in the fractures were analyzed using an X-ray energy spectrometer attached to the SEM microscope. Figure 6A presents the overview of the orthogonal face cleat and butt cleat. Figure 6B shows the non-mineralized butt cleat, where several micro-fractures exist in communication with the cleats, and the micro-pores exist on the cleat surface; Figure 6C shows the mineralized face cleat. In this situation, the adjacently mineralized and unmineralized cleats suggest a multi-stage evolutionary process for cleat formation and fluid migration during coalification. The face cleat and butt cleat in Figures 6C,D are filled with kaolinite and illite, respectively. Regarding the genesis of minerals in the coal fractures, Spears and Caswell (1986) proposed that the precipitation of sulfides first occurs at an early stage of coalification. As the coalification progressed, quartz and clay minerals precipitated one after another. Finally, the clay mineral precipitates. The adjacent cleats are filled with two different minerals, which further indicates the multi-stage evolutionary characteristic of the cleat formation and fluid migration in its geological history.

From the results, it can be observed that the original fractures normally exist as two sets: one set of fractures is almost parallel to the bedding layer plane, and these fractures are most likely hydraulic fractures which by definition form *via* a different mechanism that is unrelated to cleats. The second set of fractures is closely perpendicular to the bedding plane, which is probably cleats. The coexistence of unmineralized and mineralized fractures in the coal means that the coal seam underwent structural deformation before chemical precipitation by hydrodynamics. However, many of the open fractures originate from structural deformations during coalification. The coal-bearing basin of North China underwent three-stage orogeny. Non-sealing faults and folds with axial striking NNE–SSW and near N–S are common, which were formed by the NW–SE compressional stresses during the Jurassic–Cretaceous Yanshanian Orogeny. After undergoing Indosinian orogeny, Yanshanian orogeny, and Himalayan orogeny, many tensile faults formed during these tectonic movements.

Two mechanisms are related to the origin of coal micro-fractures: coalification and post-coalification. Coalification is the origin of endogenous micro-fractures (endo-microfracture). By contrast, the post-coalification resulting from the extraneous stress deformation induces the formation of exogenous micro-fractures (exo-microfracture). Endo-microfracture was distinctly distinguished from the exo-microfracture in the frequency and morphology of the investigated coals. As shown in Figures 6E,J, the endo-microfracture is commonly characterized by the isolated distribution, whereas the exo-microfracture is characterized by the brittle fracturing appearance such as the dendritic (Figure 6B), step-shaped (Figure 6D), filamentous (Figure 6F), and turtleback (Figure 6H) textures. More importantly, in terms of the permeability contribution, the frequency of the micro-fractures, their morphology, the connectivity of the network, and the degree of mineral filling are important controls on coal permeability. This shows that most endo-microfractures are mineralized. By contrast, most exo-microfractures are unmineralized and randomly developed by high anisotropy within the coal. The different characteristics between exo-microfracture and endo-microfracture are responsible for their different effects on coal permeability. The endo-microfracture is commonly formed within certain macerals as a result of peat formation and coalification. Based on the results of coal macerals, coal lithotype, and coal facies analyses, it was found that these factors are strongly correlated to the development of endo-microfractures. For the endo-microfractures to form, two primary preconditions must be fulfilled for coal macerals or lithotypes: the high gas generation yield together with poor gas diffusibility (Yao and Liu, 2009).

Micro-fractures related to the inorganic metallic mineral

Coal consists of a variety of inorganic constituents (minerals and nonmineral inorganics) that are broadly referred to as

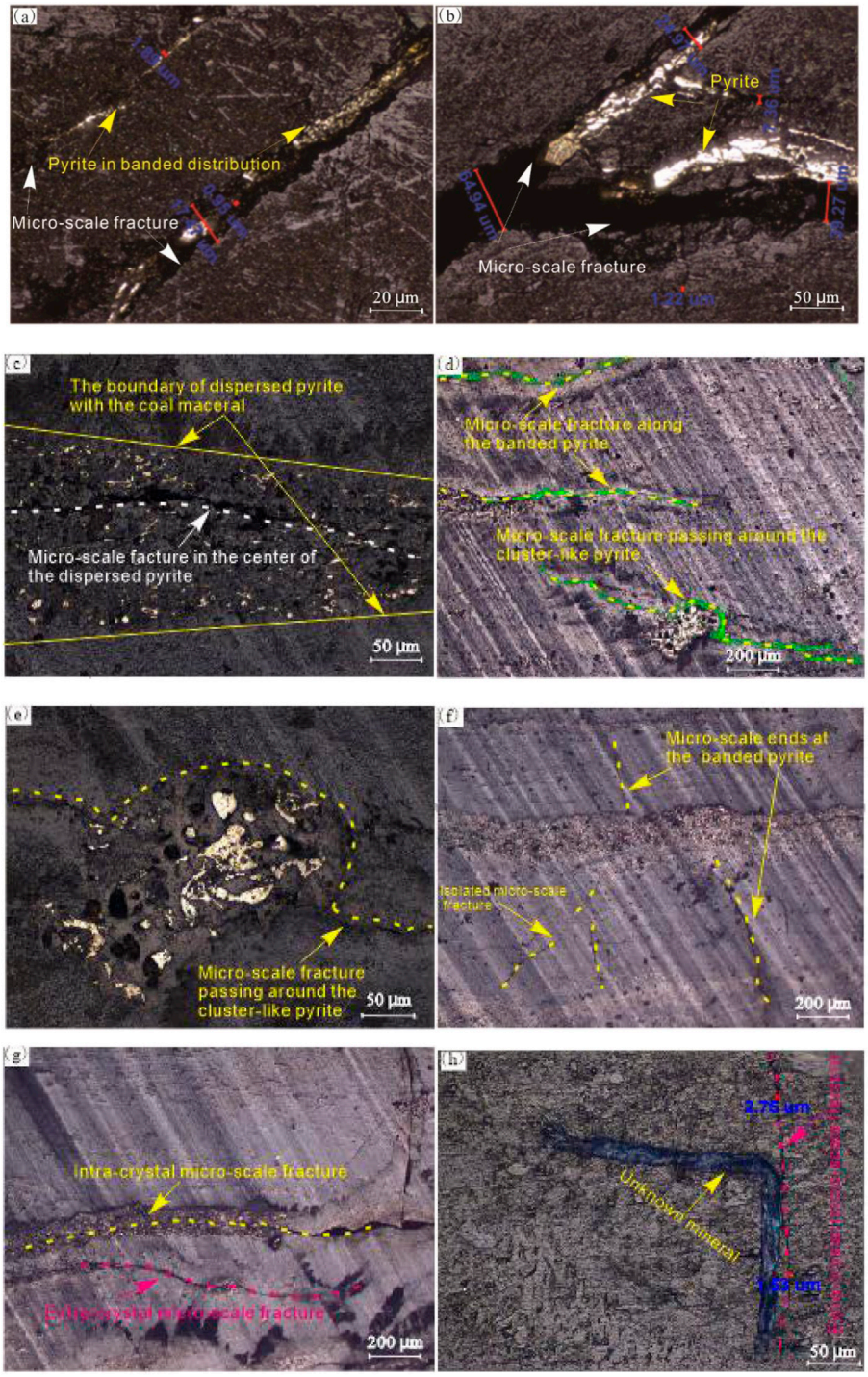

FIGURE 7
Micro-fractures to the inorganic metallic mineral: **(A)**, micro-fractures extending along the banded pyrite; **(B)**, micro-fractures bifurcated by the adjacent banded pyrite; **(C)**, micro-fractures extending along the center of the dispersed pyrite; **(D)**, micro-scale fractures extending around the edge of the cluster-like pyrite particles; **(E)**, 200-fold magnification of the Figure 7D; **(F)**, micro-fractures extending perpendicular to the banded pyrite; **(G)**, micro-fractures extending along the center of the banded pyrite; **(H)**, micro-fractures extending along with the banded mineral (unknown mineral).

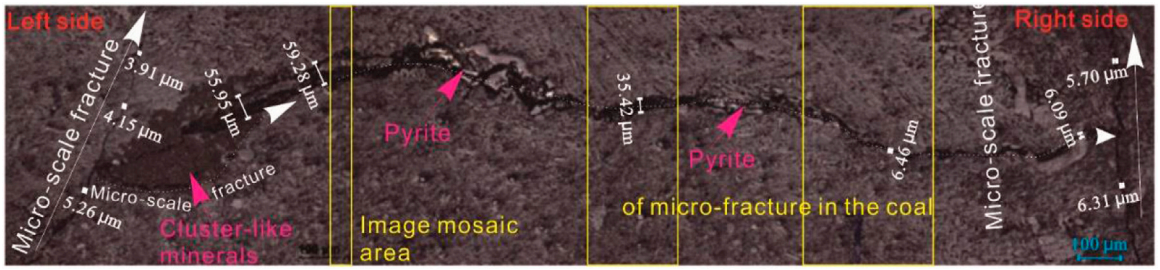

FIGURE 8
Propagation mode of micro-fracture in the coal.

mineral matter (Ward, 2002). It has been found that the extension modes of micro-fractures in coal are closely related to the occurrence of minerals. The presence of mineral matter may alter the way an induced fracture propagates through coal seams, as can the presence of pre-existing fractures. The induced fracture modes depend on the heterogeneity of the coal and the arrangement of the pre-existing macroscopic mineral bands, as well as the underground stresses. Thus, it is of great importance to study the mineral occurrence and its impact on fracture generation for CBM production.

Mineral-related micro-fractures can be classified into three types: intra-crystal micro-fractures (i.e., micro-fractures that completely developed within the mineral crystal particles), extra-crystal micro-fractures (i.e., micro-fractures that developed in the coal matrix and terminated in the mineral band or along with the mineral band), and grain edge micro-fracture (i.e., micro-fractures that developed along the edge of the particle). The mentioned three types of micro-scale fractures have been observed in the coals of SD-1, SD-2, PDS-1, and PDS-2, and their formation mechanisms were intimately associated with the occurrence form of pyrite in the coal.

Figure 7A shows the micro-fractures extending along the banded pyrite. Figure 7B shows the micro-fractures are bifurcated in the adjacent banded pyrite. Figure 7C shows the micro-fractures extending along the center of dispersed pyrite. Figure 7D shows the micro-scale fractures extending around the edge of the cluster-like pyrite particles. Figure 7E represents a 200-fold magnification of the marquee in Figure 7D to show the trace trajectory of micro-fracture development. Figure 7F shows the micro-fractures extending along the direction perpendicular to the banded pyrite. Figure 7G shows the micro-fractures extending along the center of the banded pyrite. Figure 7H shows the micro-fractures outside the crystal, and it extends along with the banded mineral (unknown mineral). Figure 8 shows the micro-fractures in the SD-1 samples. From the left view to the right view: first, the micro-fracture bifurcates at the edge of the cluster-like minerals and extends around this mineral and then extends along with the banded pyrite, eventually ending and being crossed by the vertically developed micro-fracture on the right side. The endo-microfractures are commonly formed by the processes of generation, accumulation, and centralized-release of gas from coal (Yao and Liu, 2009).

For coal, the organic compositions primarily include vitrinite maceral, liptinite maceral, and inertinite maceral. Among these, the vitrinite maceral and the liptinite maceral are brittle, whereas the inertinite maceral is somewhat ductile (Permana et al., 2013).By contrast, the mechanical properties of the organic micro-components are weaker relative to the inorganic components. The presence of inorganic micro-components in coal can cause mechanical differences between the interface of organic and inorganic components, which will make the interface boundary prone to fracturing (Li et al., 2015).

In mechanical properties, Young's modulus of pyrite is between 15 GPa and 30 GPa by the atomic force microscope contact probe testing (Cui et al., 2013). This is significantly higher than that of the coal matrix. For the pyrite present in the coal, it will improve the brittleness of the coal and affect the occurrence form of micro-fractures in the coal. At the boundary of coal maceral and pyrite, due to the differential elastic stiffness, tensile stress is formed within the pyrite particles. This finally induces the intergranular micro-fractures to be formed (Moustafa et al., 2004). In addition, due to the density difference between coal maceral and inorganic minerals, the cohesion of coal drops significantly, which makes the micro-fractures grow and extend along with the interface of coal maceral and inorganic minerals.

Micro-fractures related to the organic coal maceral

Bright coals with an abundance of brittle and fracture-prone vitrinite can become the host of many fractured flow paths during seam deformation. This makes bright coals more permeable than dull ones, which could result in more fracture-filling minerals when hydrothermal fluids or brine water flows through the seam (Permana et al., 2013). The micro-fracture development shows selectivity to the coal maceral, where the vitrinite maceral has a higher micro-fracture density for the coal, and the micro-

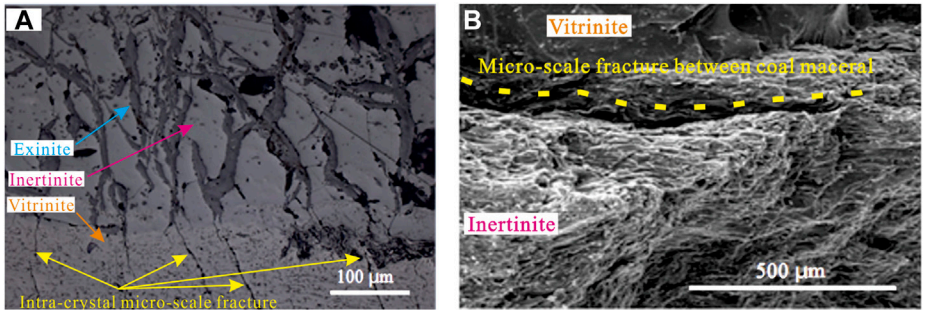

FIGURE 9
Micro-fractures developed in the coal maceral: **(A)**, vitrinite maceral; **(B)**, inertinite macerals.

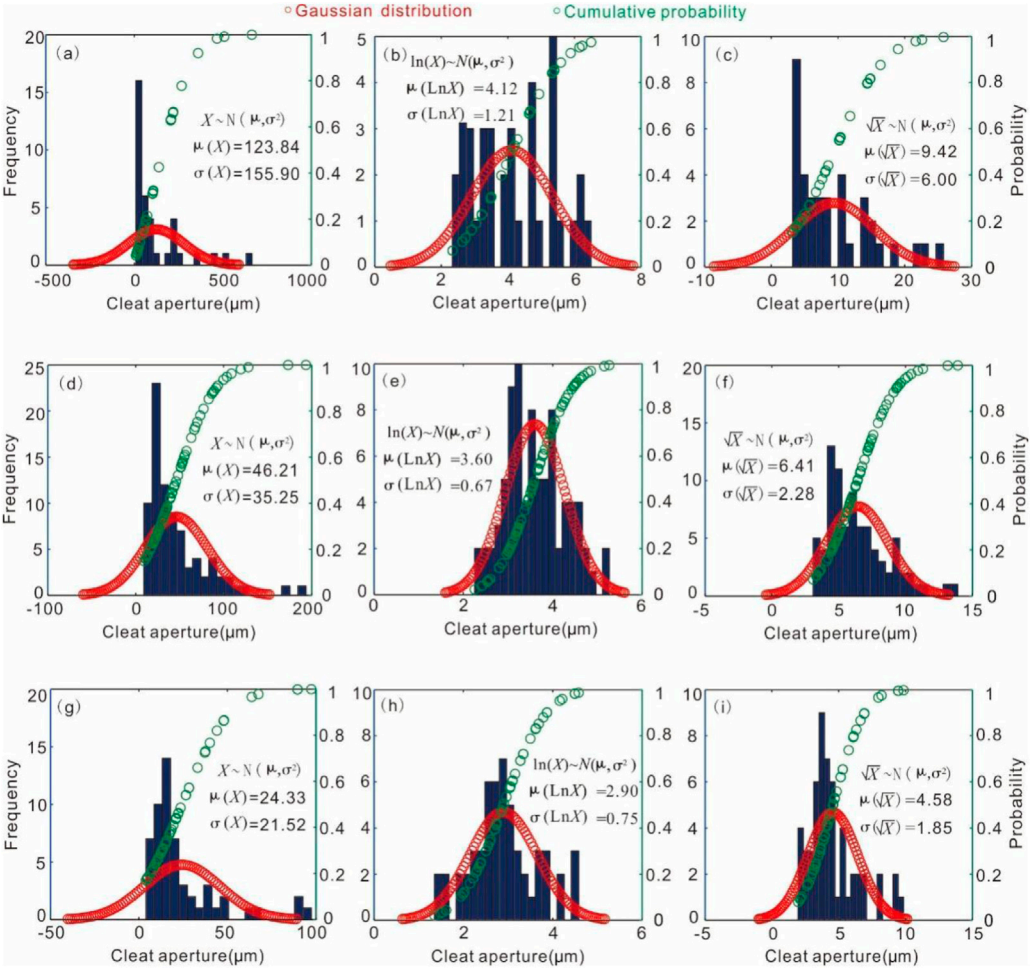

FIGURE 10
Cleat aperture distribution for the coals with different ranks: **(A–C)**, low-ranking coal; **(D–F)**, middle-ranking coal; **(G–I)**, high-ranking coal.

TABLE 4 Summary of fracture aperture goodness-of-fit statistics of coal with different ranks.

Fracture type	Coal sample	Statistical analysis	Expected aperture (μm)		Skewness (*S*)	Kurtosis (*K*)	Confidence	Interval probability		Quartile	Abundance
			Mean	Interval				P_1^{Cf}	P_2^{Cf}		
Cleat	Low-ranking coal	$x \sim N(\mu, \sigma^2)$	123.84	71.86–175.82	1.91	6.18	0.95	43.9%	87.1%	206.78	4–7 (5 cm)
		$Ln(x) \sim N(\mu, \sigma^2)$	4.12	3.72–4.53	0.28	1.89	0.95	65.5%	90.3%	206.43	
		$\sqrt{x} \sim N(\mu, \sigma^2)$	9.42	7.42–11.42	1.07	3.30	0.95	53.8%	90.6%	206.78	
	Middle-ranking coal	$x \sim N(\mu, \sigma^2)$	27.30	23.17–31.43	1.64	5.78	0.95	100%	100%	35.23	5–14 (5 cm)
		$Ln(x) \sim N(\mu, \sigma^2)$	3.11	2.98–3.25	0.35	2.40	0.95	100%	100%	35.16	
		$\sqrt{x} \sim N(\mu, \sigma^2)$	4.97	4.62–5.33	0.95	3.44	0.95	100%	100%	35.23	
	High-ranking coal	$x \sim N(\mu, \sigma^2)$	24.32	18.51–30.14	1.96	6.40	0.95	100%	100%	27.78	4–10 (5 cm)
		$Ln(x) \sim N(\mu, \sigma^2)$	2.90	2.69–3.10	0.27	2.86	0.95	99.8%	100%	27.66	
		$\sqrt{x} \sim N(\mu, \sigma^2)$	4.58	4.08–5.09	1.20	4.08	0.95	99.8%	100%	27.77	
Micro-fracture	Low-ranking coal	$x \sim N(\mu, \sigma^2)$	5.38	3.93–6.83	3.58	17.57	0.95	47.6%	99.1%	5.30	3–9 (200 μm)
		$Ln(x) \sim N(\mu, \sigma^2)$	1.33	1.14–1.51	0.51	3.63	0.95	63.9%	98.3%	5.30	
		$\sqrt{x} \sim N(\mu, \sigma^2)$	2.11	1.88–2.34	2.06	8.53	0.95	55.2	99.3%	5.30	
	Middle-ranking coal	$x \sim N(\mu, \sigma^2)$	4.37	3.62–5.11	1.73	6.46	0.95	56.6%	100%	6.10	4–11 (200 μm)
		$Ln(x) \sim N(\mu, \sigma^2)$	1.06	0.86–1.27	−0.97	4.55	0.95	70.1%	96.9%	6.10	
		$Ln(x+1) \sim N(\mu, \sigma^2)$	1.46	1.34–1.60	0.10	2.62	0.95	69.0%	99.2%	6.10	
		$\sqrt{x} \sim N(\mu, \sigma^2)$	1.91	1.74–2.08	0.61	3.29	0.95	65.0%	99.8%	6.11	
	High-ranking coal	$x \sim N(\mu, \sigma^2)$	4.22	3.27–5.17	4.08	23.62	0.95	56.1%	100%	5.51	3–7 (200 μm)
		$Ln(x) \sim N(\mu, \sigma^2)$	0.97	0.78–1.17	−0.91	5.50	0.95	72.7%	97.3%	5.50	
		$Ln(x+1) \sim N(\mu, \sigma^2)$	1.40	1.28–1.52	0.57	3.90	0.95	72.2%	99.3%	5.50	
		$\sqrt{x} \sim N(\mu, \sigma^2)$	1.83	1.66–2.01	1.68	8.25	0.95	66.7%	99.8%	5.50	

For cleats, P_1^{Cf} and P_2^{Cf} are the probability of aperture sizes less than 100 μm and 300 μm, respectively; for micro-fractures, P_1^{Mf} and P_2^{Mf} are the probability of aperture sizes less than 5 μm and 20 μm, respectively. Determination for the goodness-of-fit statistics model of aperture size distribution depending on whose kurtosis deviates little from value of K=3 and skewness deviates little from value of S=0.

10.3389/feart.2022.1048042

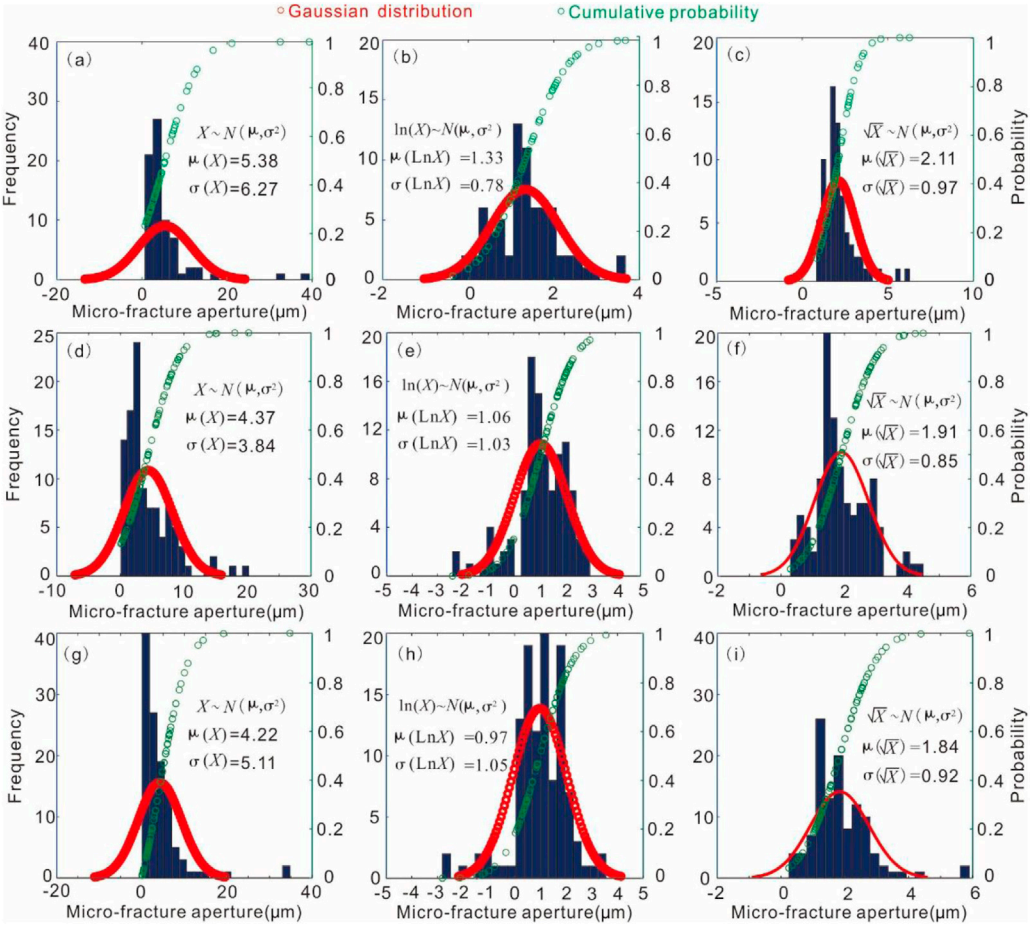

FIGURE 11
Micro-fracture aperture distribution for the coals with different ranks: **(A–C)**, low-ranking coal; **(D–F)**, middle-ranking coal; **(G–I)**, high-ranking coal.

fractures in the vitrinite maceral are interrupted at the location of their intersections to the liptinite and inertinite macerals (Figure 9A). Micro-fractures are prone to being formed along with the interface of coal maceral (Figure 9B).

For lignite of a low coal ranking, there is no self-generating high-pressure fluid. With the increase in metamorphic degree, especially in the middle-rank coal, there is more fluid in the coal pores. This decreases the liquid phase and increases the gas phase. Meanwhile, the porosity of coal decreases with the increase of metamorphic degree and the pore structure deteriorates, which hinders fluid expulsion out of the coal pores. Thus, the capillary pressure due to the existing gas-liquid two-phase fluid in the coal pores produces the local high pressure in the coal. This phenomenon forms a better choice for the vitrinite maceral, which has a high abundance of organic matter and a high potential for hydrocarbon generation. Consequently, vitrinite maceral carries more micro-fractures and endogenous fractures.

Statistical analysis of cleat and micro-fracture aperture and their permeabilities

Aperture distribution of cleat and micro-fracture

Figure 10 plots the aperture distribution for the cleat aperture of coals with different ranks. Figures 10A–C present the aperture frequency *versus* the normal distribution, the log-normal distribution, and the square root-normal distribution for the low-rank coal, respectively. Similarly, Figures 10D–F and Figures 10G–I plot the aperture frequency of cleat for the middle-rank coal and the high-rank coal, respectively. The statistical cylindrical diagram displays the aperture distributions of the cleat in the coal of different ranks are somewhat skewed. The determination

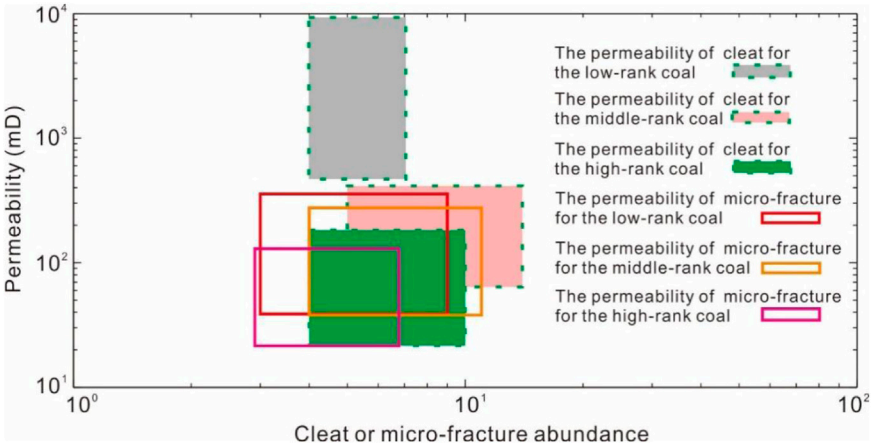

FIGURE 12
Permeability of cleat and micro-fracture for the coals of different ranks based on Weniger et al. (2016).

of the goodness-of-fit statistics model of aperture size distribution depends on four parameters as the mean value (μ), standard deviation (σ), kurtosis coefficient (K), and skewness coefficient (S). For the mean value (μ) and the standard deviation (σ) in the normal distribution and the square root-normal distribution cylindrical diagram, the cleat aperture will be negative for its two standard deviations from the mean value. Furthermore, their kurtosis coefficients and skewness coefficients deviate more from the value of K=3 and S=0, which constitute a standard for meeting a standard normal distribution (Table 4). This shows that the lognormal distribution can better descript the cleat aperture attribute, which is similar to the distribution law of fractures found in the rock (Snow, 1968). Comparingthe statistical results, cleat aperture attributes are further examined to determine the relationship between cleat aperture and coal rank. The statistical results show that the cleat apertures of low-, middle-, and high-ranking coals range from 41.26 to 92.76 μm, 19.69 to 25.79 μm, and 14.73 to 22.19 μm, respectively. Most cleat apertures are smaller than 300 μm. With the increase in coal ranking, the cleat aperture presents a decreasing trend.

Figure 11 plots the aperture distribution for the micro-fracture aperture field of coals with different ranks. Figure 11A plots aperture frequency *versus* the normal distribution of micro-fracture aperture size for low-ranking coal; and Figure 11B plots aperture frequency *versus* the lognormal distribution of micro-fracture aperture size for low-ranking coal. Figure 11C plots aperture frequency *versus* the square root-normal distribution of micro-fracture aperture size for low-ranking coal. As such, Figures 11D–F and Figures 11G–I plot the corresponding aperture frequency for middle-ranking coal and high-ranking coal, respectively. The aperture size of the micro-fracture is lower than that of the cleat by approximately an order of magnitude, and the aperture distributions are also somewhat skewed. The statistical cylindrical diagram shows that the log-normal distribution can best describe the micro-fracture aperture attribute. Determination from the skewness coefficient, data in the middle-rank coal and the high-rank coal appear to be square root-normally distributed. Actually, due to the nano-scale fracture present in the coal (88.2, 89.0, 171.2, 322.7, 400.1, 427.8, 515.8, and 639.5 nm in middle-ranking coal and 63, 230.5, 285.8, 305.6, 368.4, 456.8, 610, 630, and 712.4 nm in high-ranking coal), with an aperture size of less than 1 μm (i.e., 1000 nm) and this leads to the occurrence of negative skewness for the log-normal distribution in the unit of microns. As the data were treated as $Ln(x+1) \sim N(\mu, \sigma^2)$, the goodness-of-fit statistics of micro-fracture aperture attribute by the lognormal distribution was achieved.

Permeability of cleat and micro-fracture

Though cleat and micro-fracture apertures in the subsurface are smaller than in unstressed surface samples, they can approximate the aperture (Weniger et al., 2016). On the assumption that the cleat and micro-fracture are unmineralized and parallel each other, the permeability of cleat and micro-fracture for the coal of different ranks is evaluated from the measured abundance and apertures according to Eq. 1, as shown in Figure 12. It can be seen that the permeability of cleats for the low-, middle-, and high-ranking coal are 474–9440, 64o406, and 22o184 mD, respectively. The permeability of micro-fracture for the low-, middle-, and high-ranking coal are 39–353, 38–275, and 22–134 mD, respectively. Generally, for low-ranking coal, due to the differential aperture size, the cleat contributes more to the reservoir permeability than micro-fractures. For middle- and high-ranking coals, the contributions of cleats and micro-fractures to the coal reservoir permeability are similar. With the increase of coal rank, the cleat in the roles of contributing to the

reservoir permeability decreases, whereas the contribution of the micro-fracture to the reservoir permeability increases.

In the field, evaluated from the well test, the reservoir permeability of low-ranking coal in the Powder River Basin, America, falls at 10 to 1000 mD, that of low-ranking coal in the Surat Basin, Australia, falls at 1 to 1600 mD, that of middle- and high-ranking coals in the Bowen Basin, Australia, falls in 1–500 mD, and that of high-ranking coal in the Qinshui Basin, China, falls at 20–1.76 mD (Long et al., 2014; Kang et al., 2017). Generally, the *in situ* coal reservoir permeability for Australia and America is comparable with statistically evaluated permeability in Figure 12, with a difference of about an order of magnitude. However, the *in situ* coal reservoir permeability of China is lower than that of Australia and America by approximately 1–3 orders of magnitude. According to Tang (2001), due to the strong orogeny, the minimum geo-stress for the coal basin in China is close to the maximum geo-stress in Australia and America. Among possible reasons for the extremely low permeability of coal reservoirs in China are two aspects: 1) the subsurface cleat and micro-fracture close their apertures significantly due to the much larger geo-stress, which reduces the contribution of cleat and micro-fracture to the coal reservoir permeability; 2) the subsurface cleat and micro-fracture have better permeability for the hydrothermal fluids in the geological history, which is beneficial to the precipitation of minerals in the stressed cleat and micro-fracture and thereby the decreased coal reservoir permeability.

Implications of cleat and micro-fracture to the field CBM exploration and exploitation

Cleat and micro-fracture apertures in conjunction with spacing and degree of mineralization define the permeability of coal reservoirs. To stimulate gas production, hydraulic fracturing is a means of creating more fractures for fluid flow, which includes newly created fractures and increased sizes of openings of the existing ones. The mineral in the coal can change the mechanical and petrophysical features of the coal seam, which determines the growth of created fractures. In addition, the mineral matter in coal, especially the massive clay minerals and carbonate minerals, is a significant aspect in the design and selection of fluids for drilling and hydraulic fracturing. Nowadays, acid treatment is extensively used in sandstone reservoirs to remove the formation damage (Shuchart and Gdanski, 1996; Taylor et al., 2005; Yang et al., 2012; Zhang et al., 2017). In terms of the common mineral occurrences in cleats and micro-fractures in coal, acid solvents such as HAc, HCl, and HF at a certain concentration can be added to the drilling or hydraulic fracturing fluid to remove the minerals and enhance the reservoir permeability. Meanwhile, geo-stress relief technologies may be also an effective way of enlarging the cleat or micro-fracture aperture for enhancing the coal reservoir permeability (Du et al., 2022).

Conclusion

1) The neighboring mineralized and unmineralized cleats suggest multi-stage evolution processes for cleat formation during the process of coalification. The micro-fracture distribution of coals is closely related to their components, including organic macerals and inorganic minerals. Generally, micro-fractures have a high density in the vitrinite maceral and develop more at the junction surface of organic macerals or the surface between the organic and inorganic minerals. The formation mechanism of mineral-genetic micro-fractures can be classified as intra-crystal micro-fractures, extra-crystal micro-fractures, and grain edge micro-fractures. Compared with the low- and middle-ranking coals, cleats and micro-fractures in high-ranking coal are usually filled with carbonate minerals and clay minerals.
2) Statistical analysis reveals that the aperture distribution of cleats and micro-fractures in coal meets a log-normal distribution. The aperture of cleat and micro-fracture in the coal shows a decreasing trend with the increase of coal rank. Given the assumptions that the cleat and micro-fracture are unmineralized and parallel each other, the permeability of cleats for the low-, middle-, and high-ranking coals is 474–9440 mD, 64 to 406 mD, and 22 to 184 mD, and the permeability of micro-fractures for the low-, middle-, and high-ranking coals is 39–353 mD, 38 to 275 mD, and 22 to 134 mD, respectively. For the low-ranking coal, cleat contributes more to the reservoir permeability than micro-fractures do. For the middle- and high-ranking coal, the contribution of cleat and micro-fracture to the coal reservoir permeability will be close. With the increase in coal ranking, the degree of cleat contributing to reservoir permeability decreases, whereas that of micro-fractures contributing to the reservoir permeability increases.
3) Among the possible reasons for the extremely low permeability of coal reservoirs in China may be two aspects: one is that the subsurface cleats and micro-fractures close their apertures significantly due to the *in situ* geo-stress; the other is that subsurface cleats and micro-fractures have better permeability for the hydrothermal fluids in the geological history, which increases the precipitation of minerals in the cleat and micro-fracture and then decreases the coal reservoir permeability.

4) Regarding the mineral presenting in the cleat and micro-fracture of coal, acid solvents (e.g., HAc, HCl, and HF) can be added to the drilling or hydraulic fracturing fluid to remove the minerals for enhancing the reservoir permeability. In addition, the geo-stress relief technologies may also be an effective way to improve the coal reservoir permeability for CBM production.

Data availability statement

The original contributions presented in the study are included in the article/Supplementary Material; further inquiries can be directed to the corresponding author.

Author contributions

QH and ZD were responsible for the experiments and the writing of this manuscript. HL, QN, and HF helped create the figures for this paper. JY and ML provided language help. Each author has contributed to this manuscript.

Funding

This study has been sponsored financially by the Natural Science Foundation of Henan Province (Project no. 222300420242), the Science and Technology Development Project of Luoyang (Project no. 2101025A), the Heluo Young Talent Lifting Project of Society and Technology Association of Luoyang (Project no. 2022HLTJ06), the Science and Technology Innovation Leading Talent Project of Zhongyuan (Project no. 214200510030), and the Key Research and Development Project of Henan Province (Project no. 221111321500).

Acknowledgments

We are grateful to the reviewers for their suggestions for improving this paper.

Conflict of interest

ZD was employed by Yima Coal Corporation, Henan Energy Group Corporation.

The remaining authors declare that the research was conducted in the absence of any commercial or financial relationships that could be construed as a potential conflict of interest.

Publisher's note

References

Brixel, B. (2020). *Fluid flow in sparse fracture systems, prior to and after fault slip (PhD thesis)*. Zürich: ETH Zürich.

Cui, J. W., Zhu, R. K., Wu, S. T., and Bai, B. (2013). The role of pyrite in shale organic matter enrichment, hydrocarbon generation and expulsion and shale oil accumulation. *Geol. Rev.* 59, 783–784.

Dai, S. F., Luo, Y., Seredin, V. V., Ward, C. R., Hower, J. C., Zhao, L., et al. (2014). Revisiting the late Permian coal from the Huayingshan, Sichuan, southwestern China: enrichment and occurrence modes of minerals and trace elements. *Int. J. Coal Geol.* 122, 110–128. doi:10.1016/j.coal.2013.12.016

Du, Z. G., Tao, Y. W., Zhang, X. D., Ding, W. X., and Huang, Q. (2022). CBM exploration: permeability of coal owing to cleat and connected fracture. *Energy Explor. Exploitation* 40 (1), 38–56. doi:10.1177/01445987211057195

Du, Z. G., Zhang, X. D., Huang, Q., Zhang, S., and Wang, C. (2019). Investigation of coal pore and fracture distributions and their contributions to coal reservoir permeability in the Changzhi block, middle-southern Qinshui Basin, North China. *Arab. J. Geosci.* 12, 505–519. doi:10.1007/s12517-019-4665-9

Gamson, P. D., Beamish, B. B., and Johnson, D. P. (1993). Coal microstructure and micropermeability and their effects on natural gas recovery. *Fuel* 72, 87–99. doi:10.1016/0016-2361(93)90381-b

Golab, A., Ward, C. R., Permana, A., Lennox, P., and Botha, P. (2013). Highresolution three-dimensional imaging of coal using microfocus Xray computed tomography, with special reference to modes of mineral occurrence. *Int. J. Coal Geol.* 113, 97–108. doi:10.1016/j.coal.2012.04.011

Gong, W. L., An, L. Q., Zhao, H. Y., and Mao, L. T. (2010). Multiple scale characterization of CT image for coal rank fractures based on image description. *Rock Soil Mech.* 31, 371–381.

Heriawan, M. N., and Koike, K. (2015). Coal quality related to microfractures identified by CT image analysis. *Int. J. Coal Geol.* 140, 97–110. doi:10.1016/j.coal.2015.02.001

Kang, Y. S., Sun, L. Z., Zhang, B., Jiao, G. U., Jian, Y. E., jiang, S., et al. (2017). The controlling factors of coalbed reservoir Permeability and CBM development strategy in China. *Geol. Rev.* 63 (5), 1401–1418.

Karacan, C., and Okandan, E. (2000). Fracture/cleat analysis of coals from Zonguldak Basin (northwestern Turkey) relative to the potential of coalbed methane production. *Int. J. Coal Geol.* 44, 109–125. doi:10.1016/s0166-5162(00)00004-5

Kendall, P. F., and Briggs, H. (1933). XIII.—the Formation of rock joints and the cleat of coal. *Proc. R. Soc. Edinb.* 53, 164–187. doi:10.1017/s037016460001556x

Kumar, H., Lester, E., Kingman, S., Bourne, R., Avila, C., Jones, A., et al. (2011). Inducing fractures and increasing cleat apertures in a bituminous coal under isotropic stress via application of microwave energy. *Int. J. Coal Geol.* 88 (1), 75–82. doi:10.1016/j.coal.2011.07.007

Laubach, S. E., Marrett, R. A., Olson, J. E., and Scott, A. R. (1998). Characteristics and origins of coal cleat: a review. *Int. J. Coal Geol.* 35, 175–207. doi:10.1016/s0166-5162(97)00012-8

Li, C. C., Liu, D. M., Pan, Z. J., and Pan, Z. J. (2015). Mineral occurrence and its impact on fracture generation in selected Qinshui Basin coals: An experimental perspective. *Int. J. Coal Geol.* 150-151, 35–50. doi:10.1016/j.coal.2015.08.006

Long, S. X., Ye, L. Q., and Chen, C. F. (2014). Comparison and enlightenment of coalbed methane geology at home and abroad. *QilGas Geo* 35 (5), 696–703.

Mohamad, N. H., and Katsuaki, K. (2015). Coal quality related to microfractures identified by CT image analysis. *Int. J. Coal Geol.* 140, 97–110. doi:10.1016/j.coal.2015.02.001

Moustafa, E. O., Tang, C. A., and Zhang, Z. (2004). Scanning of essential minerals in granite electron microscope study on the microfracture behavior. *Geo. Resour.* 13, 129–136.

Nalendra, J. S., Edy, S., and Dyah, H. E. W. (2020). "Coal properties and cleat attributes at TanjungEnim coalfield in south palembang sub-basin, south sumatra," in AIP Conference Proceedings, 2nd International Conference on Earth Science, Mineral, and Energy, China, 08 July, 2020.

Niu, Q. H., Wang, Q. Z., Wang, W., Chang, J. F., Chen, M. Y., Wang, H. C., et al. (2021). Responses of multi-scale microstructures, physical-mechanical and hydraulic characteristics of roof rocks caused by the supercritical CO_2-water-rock reaction. *Energy* 238, 121727. doi:10.1016/j.energy.2021.121727

Olson, J. E., Laubach, S. E., and Lander, R. H. (2009). Natural fracture characterization in tight gas sandstones: Integrating mechanics and diagenesis. *Am. Assoc. Pet. Geol. Bull.* 93 (11), 1535–1549. doi:10.1306/08110909100

Pan, J. N., Wang, H. C., Wang, K., and Niu, Q. (2014). Relationship of fractures in coal with lithotype and thickness of coal lithotype. *Geomech. Eng.* 6 (6), 613–624. doi:10.12989/gae.2014.6.6.613

Permana, A., Ward, C. R., Li, Z., and Gurba, L. W. (2013). Distribution and origin of minerals in high-rank coals of the south walker creek area, Bowen Basin, Australia. *Int. J. Coal Geol.* 116-117, 185–207. doi:10.1016/j.coal.2013.03.001

Rutqvist, J., Figueiredo, B., Hu, M., and Tsang, C. F. (2018). "Continuum modeling of hydraulic fracturing in complex fractured rock masses," in *Hydraulic fracture modeling* (Netherland: Elsevier), 195–217.

Sapiie, B., Rifiyanto, A., and Perdana, L. A. (2014). "Cleats analysis and CBM potential of the barito basin, south kalimantan, Indonesia," in AAPG International Conference & Exhibition, Istanbul, Turkey, September 14-17.

Saxby, J. D. (2000). "Minerals in coal," in *Organic matter and mineralisation: Thermal alteration, hydrocarbon generation and role in metallogenesis*. Editors M. Mastalerz and M. Glikson (New York: Kluwer Academic Publishers), 314–328.

Scott, A. R. (2002). Hydrogeologic factors affecting gas content distribution in coal beds. *Int. J. Coal Geol.* 50 (1-4), 363–387. doi:10.1016/s0166-5162(02)00135-0

Shi, X. H., Pan, J. N., Hou, Q. L., Jin, Y., Wang, Z. Z., Niu, Q. H., et al. (2018). Micrometer-scale fractures in coal related to coal rank based on micro-CT scanning and fractal theory. *Fuel* 212, 162–172. doi:10.1016/j.fuel.2017.09.115

Shuchart, C. E., and Gdanski, R. D. (1996). "Improved success in acid stimulation with a new organic-HF system," in Presented at European Petroleum Conference, Milan, Italy, Oct 22-24.

Snow, D. T. (1968). Rock fracture spacings, openings, and porosities. *J. Soil Mech. Found. Div.* 94, 73–91. doi:10.1061/jsfeaq.0001097

Solano, W., Mastalerz, M., and Schimmelmann, A. (2007). Cleats and their relation to geologic lineaments and coalbed methane potential in Pennsylvanian coals in Indiana. *Int. J. Coal Geol.* 72, 187–208. doi:10.1016/j.coal.2007.02.004

Spears, D. A., and Caswell, S. A. (1986). Mineral matter in coals: cleat minerals and their origin in some coals from the english midlands. *Int. J. Coal Geol.* 6, 107–125. doi:10.1016/0166-5162(86)90015-7

Tang, S. H. (2001). Probe into the influence factors on permeability of coal reservoirs. *Coal Geo. China.* 13 (1), 28–31.

Taylor, K. C., Al-Katheeri, M. I., Nasr-EI-Din, H. A., and Aramco, S. (2005). Development and field application of a new measurement technique for organic acid additives in stimulation fluids. *SPE J.* 10, 152–160. doi:10.2118/85081-pa

Wang, Z., Fu, X., Hao, M., Li, G., Pan, J., Niu, Q., et al. (2021). Experimental insights into the adsorption-desorption of CH_4/N_2 and induced strain for medium-rank coals. *J. Pet. Sci. Eng.* 204, 108705. doi:10.1016/j.petrol.2021.108705

Wang, Z., Pan, J., Hou, Q., Yu, B., Li, M., and Niu, Q. (2018). Anisotropic characteristics of low-rank coal fractures in the Fukang mining area, China. *Fuel* 211, 182–193. doi:10.1016/j.fuel.2017.09.067

Ward, C. R. (2002). Analysis and significance of mineral matter in coal seams. *Int. J. Coal Geol.* 50, 135–168. doi:10.1016/s0166-5162(02)00117-9

Ward, C. R. (2016). Analysis, origin and significance of mineral matter in coal: an updated review. *Int. J. Coal Geol.* 165, 1–27. doi:10.1016/j.coal.2016.07.014

Weniger, S., Weniger, P., and Littke, R. (2016). Characterizing coal cleats from optical measurements for CBM evaluation. *Int. J. Coal Geol.* 154-155, 176–192. doi:10.1016/j.coal.2015.12.005

Yang, F., Nasr-EI-Din, H. A., and Al-Harbi, B. M. (2012). "Acidizing sandstone reservoirs using HF and formic acids," in Presented at the SPE International Symposium and Exhibition on Formation Damage Control, Lafayette, Louisiana, Feb 15-17.

Yao, Y. B., Liu, D. M., Cai, Y. D., and Li, J. Q. (2010). Advanced characterization of pores and fractures in coals by nuclear magnetic resonance and X-ray computed tomography. *Sci.Sinic. Terr.* 40, 1598–1607. doi:10.1007/s11430-010-0057-4

Yao, Y. B., and Liu, D. M. (2009). Microscopic characteristics of microfractures in coals: An Investigation into permeability of coal. *Procedia Earth Planet. Sci.* 1, 903–910. doi:10.1016/j.proeps.2009.09.140

Zhang, X. D., Yu, K. K., Zhang, S., and Du, Z. G. (2017). Change mechanism in surface properties of treated tectonic coal by different acids. *Coal Convers.* 40, 1–7.

Zhang, Y. H., Xu, X. M., Lebedev, M., Sarmadivaleh, M., Lglauer, S., and Iglauer, S. (2016). Multi-scale x-ray computed tomography analysis of coal microstructure and permeability changes as a function of effective stress. *Int. J. Coal Geol.* 165, 149–156. doi:10.1016/j.coal.2016.08.016